

See discussions, stats, and author profiles for this publication at: <http://www.researchgate.net/publication/227000163>

The Maunder minimum: North-south asymmetry in sunspot formation, mean sunspot latitudes, and the butterfly diagram

ARTICLE *in* ASTRONOMY REPORTS · MAY 2010

Impact Factor: 0.94 · DOI: 10.1134/S1063772910050112

CITATIONS

9

READS

19

4 AUTHORS, INCLUDING:



[Yu. A. Nagovitsyn](#)

Pulkovo observatory of the Russian Academy...

108 PUBLICATIONS 522 CITATIONS

[SEE PROFILE](#)

The Maunder Minimum: North–South Asymmetry in Sunspot Formation, Mean Sunspot Latitudes, and the Butterfly Diagram

Yu. A. Nagovitsyn, V. G. Ivanov, E. V. Miletsky, and E. Yu. Nagovitsyna

General Astronomical Observatory at Pulkovo, Russian Academy of Sciences,
Pulkovo, St. Petersburg, 196140 Russia

Received November 11, 2009; in final form, November 26, 2009

Abstract—An approach to reconstructing solar activity in the past is used to study its time evolution. It is already possible to reconstruct not only the general level of solar activity on long timescales, but also particular aspects of its development: sunspot dominance in either hemisphere, the drift and latitude spread of the sunspot-formation zone, and features in the spatial distribution of the activity at specific epochs, such as the Maunder minimum.

DOI: 10.1134/S1063772910050112

1. INTRODUCTION

The course of solar activity (SA) can be represented as a process of *quasi-periodic* variations in the *global* magnetic field of the Sun on *various timescales*.

The word quasi-periodic stresses the nonstationary character of cyclic components in SA. The word global states the fact that, in addition to the sunspot cycle, the Sun has a cycle of its large-scale (background) magnetic field formed by open configurations (coronal holes), as well the polar field formed by polar coronal holes and polar faculae. The various timescales for variations in the global magnetic field and its components include a number of other long-term cycles, apart from the 11-year Schwabe–Wolf cycle known for more than one and half centuries: the ~80–90-year Gleissberg cycle, 200-year Suess cycle, 900-year cycle, and even longer cycles. All these long-duration cycles are related to the amplitude-modulation (and, probably, frequency-modulation) of the 11-year cycles, and result in a nontrivial pattern of SA, which includes huge extrema: the minima associated with Maunder, Dalton, Spörer, Wolf, etc., as well as maxima — Medieval, Late Medieval, Modern (middle–end of the 20th century), etc.

The actual development of SA in different hemispheres of the Sun displays a multitude of interesting features (such as “sympathetic” cross-equatorial manifestations and others). However, the general pattern is described by the so-called Maunder butterfly diagram, due to the characteristic drifts of the mean latitude and variations in the latitude spread of sunspot formation zones with a period of ~11 years. We consider here precisely these aspects, concentrating mainly on the reconstruction of the

spatial behavior of SA at the epoch of the Maunder minimum. We use annual average values for our analysis.

We used the “Extended time series of Solar Activity Indices” (ESAI) database available on the site www.gao.spb.ru/database/esai as reference observations. Our paper [1] describes this database. The available data about parameters of solar cyclicity were supplemented by several long-term series of indices of various SA components obtained by reconstructing early 19th-century observations of various authors and compiling these in databases. In total, we obtained six new series, which cover a time interval ~50% longer than the series that are usually used: (a) total sunspot areas in the Greenwich system (1821–1995), (b) average sunspot latitudes (1854–1989), (c) “synthetic” series of the numbers of polar faculae in the Mount Wilson system (1847–1999), (d, e, f) north–south asymmetry in the indices (a, b, c). We will specify other data utilized in this study in the text.

Let us first consider north–south asymmetry as an SA index.

2. NORTH–SOUTH ASYMMETRY OF SUNSPOT FORMATION

The north–south (NS) asymmetry of activity is a special parameter of the spatial organization of SA. It is defined most frequently as [2]:

$$\langle AS \rangle \equiv q = (N - S)/(N + S), \quad (1)$$

where N and S are the values of selected SA indices in the northern and southern hemispheres. The NS asymmetry is sometimes defined as $Q =$

N/S. Selected indices may include not only indices of sunspot-formation power, but also the observed average sunspot latitudes, number of polar faculae [1], number of coronal mass ejections [3], area of facula areas (e.g., in the K CaII line [4]), coronal brightness in lines [5], etc. We will consider here the traditional asymmetry index defined in (1) based on the total sunspot area in the N and southern hemispheres of the Sun.

In spite of efforts directed toward studies of regularities in the global temporal–spatial organization of SA, the physics and phenomenology of time variations in the NS activity asymmetry $q(t)$ remain, in many respects, unclear. Some authors, e.g., Carbonell et al. [6], question the statistical significance of this parameter, though they conclude that an exact answer to this question cannot be given. We believe that the elucidation of this problem can be aided by invoking additional data and studying various mathematical models describing the empirical picture. One example is the scheme of Waldmeier [7] linking the average position of sunspot-formation zones relative to the solar equator with a 80–90-year cycle. Oliver and Ballester [8] constructed a model of $q(t)$ based on the decomposition theorem. Zolotova and Ponyavin [9] treated the asymmetry like the development of phase asynchronism in the activity of the hemispheres.

In the current paper, we aim to quantify the activity of each hemisphere of the Sun as an independent SA index. This allows us to reconstruct the N and S activity separately using the DPS (Decomposition in pseudo-Phase Space) approach proposed by us earlier in [10], then use these reconstructions to describe the course of the NS asymmetry. However, we first present some words about this method, which has already been applied many times to reconstruction problems.

3. DECOMPOSITION IN PSEUDO-PHASE SPACE

The DPS method enables us to trace multi-scale connections between processes. It is based on the well-known approach of Takens [11]. A scalar time series (e.g., a series of any SA index) can be treated as the typical continuous projection of the phase trajectory of a dynamical system (describing the SA) as a whole. Assuming that the original system is dissipative, i.e., it has a (D -dimensional) attractor, we can use the projection to reconstruct a copy of the attractor in the \mathcal{R}^n Euclidean space ($n \geq 2D + 1$) as a topological embedding of the time series. “Embedding” means that the copy and the original attractor

coincide to within continuous transformations. According to Takens, the copy whose points are formed in \mathcal{R}^n as

$$(X(t), X(t - \Delta), X(t - 2\Delta), \dots, \\ X(t - (n - 1)\Delta)) \quad (2)$$

(Δ is a fixed time shift) conserves all main dynamical characteristics of the original.

We wish to find the connection of a process parametrized by an observed quantity (observable) $Y(t)$ with a process parametrized by the observable $X(t)$. The required values of n and Δ can be determined using the laws of nonlinear dynamics [12]. Following the main idea of the DPS method, we expand $Y(t)$ in phase-space components. Because of the shift, the number of points in the copy involving a transformation of the retarded coordinates (2) is a factor of $(n - 1)\Delta$ fewer than the initial series. In order for the beginning and end of the series to be equivalent in terms of loss of points, it is expedient to center $Y(t)$ on the middle component (2), i.e., to make a shift transformation $t \rightarrow t - (n - 1)\Delta/2$ in (2) (n is an odd number). Thus, we find on the common interval for the existence of the series expansion coefficients a_i in linear form

$$Y(t) = Y_0 + a_1 X(t + (n - 1)\Delta/2) \quad (3)$$

$$+ a_2 X(t + (n - 3)\Delta/2) + \dots$$

$$+ a_{(n+1)/2} X(t) + \dots + a_n X(t - (n - 1)\Delta/2),$$

and apply these values on the extended interval, where the values of $X(t)$ are known and those of $Y(t)$ are not. We reconstruct the behavior of $Y(t)$ based on the behavior of $X(t)$. Closeness of the model $Y(t)$ values to the observed values may indicate a successful reconstruction. Thus, using a time series of an index describing an SA process, we can find a time series of some other SA index, bearing in mind that both are produced by the same system and are therefore connected through a phase space.

Both general considerations and experience in applying the DPS method to particular problems indicate that the best results can be obtained when the reference series $X(t)$ is first linearized [10, 13]; i.e., the copy of the attractor in the n -dimensional space is formed by some simple function of $X(t)$ that provides a more uniform density of points along the basic cycle of the attractor. This is consistent with the fact that, in our implementation of the DPS method, we construct a linear form of the representation (3). Basically, the usual “inductive” methods of prediction [14] enable us to work without preliminary linearization. However, in this case, the meaning of the elegant fundamental result of Takens is somewhat blurred.

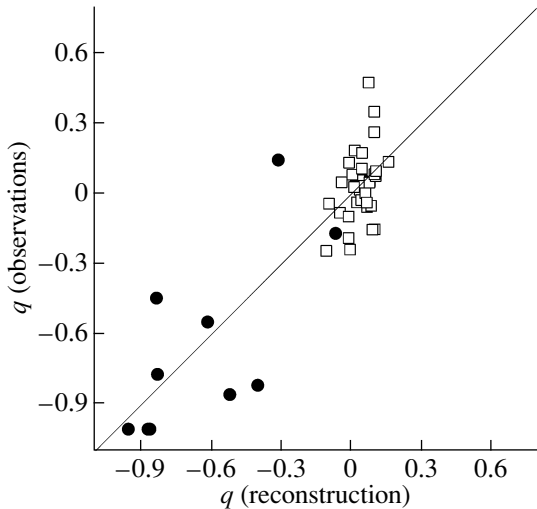


Fig. 1. Illustration of agreement of the model NS-asymmetry values to the observations. The hollow squares show the values used in the model (1821–2005) and the filled circles independent test observations during the Maunder minimum (1671–1718).

4. SUNSPOT ACTIVITY IN THE NORTHERN AND SOUTHERN HEMISPHERES OF THE SUN

As we noted above, we consider the sunspot activity of each solar hemisphere as a separate SA index and analyze the behavior of the N and S activity using the DPS method. As a reference series for the sunspot areas in the N and southern hemispheres [$Y(t)$ in (3)], we use our series from the ESAI database for 1821–1995 (see Section 1). As the reconstructing series $X(t)$, we use the last version of the series of the total sunspot area over a 400-year interval [15] with the addition of the epoch of the Maunder minimum [13]. To linearize the phase space, we took the square root of the annual average values of the area as in, e.g., [13].

The results of the reconstruction (sunspot area in the N hemisphere) are described in the interval 1821–2005 by the correlation coefficient $\rho = 0.977$, and in the S hemisphere by $\rho = 0.970$.

Let us check the values obtained using the asymmetry of the two hemispheres (1). In our reconstructions for the individual hemispheres, we did not use the values of q during the Maunder minimum from Ribes and Nesme-Ribes [16]. Let us calculate q for the reconstructed values and compare with the observations from this paper. For the five-year-averages, the correlation coefficient is $\rho = 0.702$ with regression coefficients $a = -0.06 \pm 0.23$ and $b = 0.93 \pm 0.33$ ($y = a + bx$); i.e., these are statistically indistinguishable from 0 and 1, respectively (Fig. 1). We consider this to be a good result in view of the

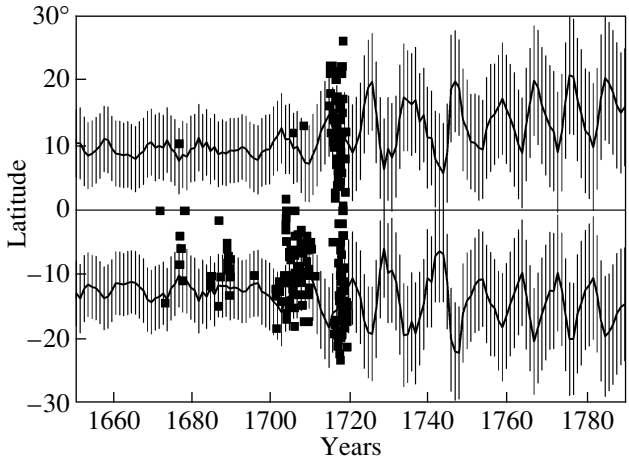


Fig. 2. Comparison of the model latitude values with independent test observations during the Maunder minimum (squares). The vertical lines show the 3σ confidence intervals of the model.

sparse information about the Maunder minimum and incomplete knowledge about the NS asymmetry in general. The total correlation coefficient between the reconstructed q values and all the observed values is 0.875.

Let us now proceed to an interesting SA index: the mean latitude of sunspot formation.

5. MEAN LATITUDE OF SUNSPOT FORMATION

The Spörer law concerns the drift of the sunspot-formation zone from latitudes 30° – 40° at the beginning to 0° – 5° at the end of the 11-year cycle; thus, the time sweep of the sunspot formation latitudes has a characteristic pattern known as the “Maunder butterflies” [2]. This fundamental law has been confirmed not only for the Sun but also, through modeling of broadband photometric data, for a number of other stars [17].

We carried out earlier in [18] a 400-year reconstruction of the average sunspot latitudes without separation into hemispheres, i.e., $\bar{\varphi} = (|\bar{\varphi}_N| + |\bar{\varphi}_S|)/2$. We will now carry out this reconstruction for the hemispheres separately ($\bar{\varphi}_N$ and $\bar{\varphi}_S$) using the DPS method and the observed values of these parameters for 1853–1984 from our ESI database.

The obtained correlation coefficients between the model and observations are $\rho = 0.833$ for the northern hemisphere and $\rho = 0.852$ for the southern hemisphere. The data on the Maunder minimum were not included.

As a test of this reconstruction, we again used the independent data of Ribes and Nesme-Ribes [16]

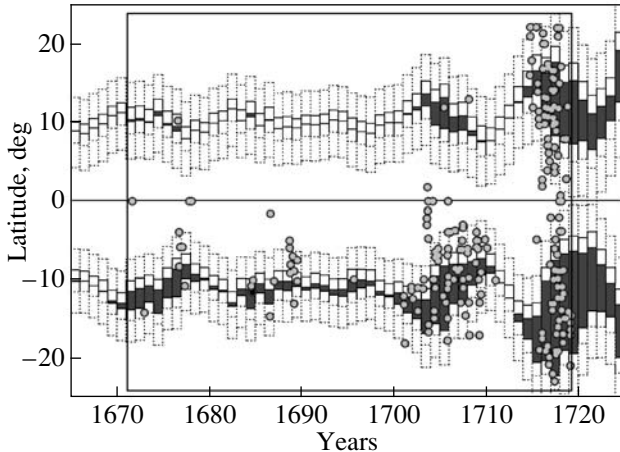


Fig. 3. Model Maunder butterflies in the global Maunder minimum of solar activity (dark areas) and a comparison with the observations of 1671–1718 (gray circles). The vertical rectangles show 1σ and 3σ confidence intervals for the model in latitude.

during the Maunder minimum (Fig. 2). Note that our reconstruction correctly reflects the average decrease in the absolute values of the latitudes when approaching this epoch. However, the reconstructed values seem to be $\sim 10\%$ greater than the observed ones. Recall that our construction for the DPS model did not use data for the Maunder minimum. Therefore, the results seem satisfactory, though for our subsequent analysis we multiplied the model latitudes for the Maunder minimum by a factor of 0.9.

6. SPATIAL DISTRIBUTION OF ACTIVITY DURING THE MAUNDER MINIMUM

We will now use the results obtained to proceed to the overall objective of this research: reconstruction of the spatial distribution of SA during the Maunder minimum.

We established in [19] for the 11-year SA cycle a tight relation between its manifestations in time (the Schwabe–Wolf law) and in space (the Spörer–Maunder law). More specifically, we showed that the width of the Maunder butterflies in the 11-year cycle depends on the current level of activity.

Applying the DPS method (to take into account the dependence on longer cycles than the 11-year mean) and using the results obtained above, we reconstructed Maunder butterfly diagrams including (and this is the main point) the deep Maunder minimum of SA. Figure 3 demonstrates a comparison of the obtained pattern with the observations according to Ribes and Nesme-Ribes [16]. We can see that our approach to this reconstruction is successful: the model pattern matches the observed pattern well, and correctly reproduces its characteristic features.

7. CONCLUSION

In this paper, we have studied the possibility of reconstructing the SA spatial distribution in the past, on a 400-year timescale. In our construction of mathematical models using the DPS method, we used only observations of the 19th–20th centuries, whereas the observation of the French school (Picard, de la Hire) in 1671–1718 summarized by Ribes and Nesme-Ribes [16] were used as comparison data. The results (shown mainly in Fig. 3) provide hope for the future development of reliable knowledge about SA variations in the past. It seems that we can now reconstruct not only the general SA level on long timescales, but also specific aspects of its development: sunspot dominance in either hemisphere, the drift and latitude spread of the sunspot-formation zone, and peculiarities in the spatial distribution of the activity at peculiar epochs such as the Maunder minimum.

ACKNOWLEDGMENTS

This work was partially supported by the Russian Foundation for Basic Research (project codes 07-02-00379 and 09-02-00083), the Program of State Support for Leading Scientific Schools of the Russian Federation (grant NSh-6110.2008.2), the Federal Agency for Science and Innovations (state contract No. 02.740.11.0246), and Basic Research Program of the Presidium of the Russian Academy of Sciences P-16.

REFERENCES

1. Yu. A. Nagovitsyn, V. G. Ivanov, E. V. Miletsky, and D. M. Volobuev, *Solar Phys.* **224**, 103 (2004).
2. Yu. I. Vitinsky, M. Kopetsky, and G. V. Kuklin, *Statistics of Spot Formation Activity of the Sun* (Nauka, Moscow, 1986) [in Russian].
3. Su-Lyun Rho and Heon-Young Chang, *J. Astron. Space Sci.* **26**, 009 (2009).
4. I. Dorotovic, P. Journoud, J. Rybak, and J. Sykora, *ASP Conf. Ser.* **368**, 527 (2007).
5. O. G. Badalyan, V. N. Obrikko, Ya. Rybak, and Yu. Sikora, *Astron. Zh.* **82**, 740 (2005) [*Astron. Rep.* **49**, 659 (2005)].
6. M. Carbonell, J. Terradas, R. Oliver, and J. L. Ballester, *Astron. Astrophys.* **476**, 951 (2007).
7. M. Waldmeier, *Z. Astrophys.* **43**, 149 (1957).
8. R. Oliver and J. L. Ballester, *Solar Phys.* **169**, 215 (1996).
9. N. V. Zolotova and D. I. Ponyavin, *Astron. Astrophys.* **449**, L1 (2006).
10. Yu. A. Nagovitsyn, *Pis'ma Astron. Zh.* **32**, 382 (2006) [*Astron. Lett.* **32**, 344 (2006)].

11. F. Takens, Lect. Notes Math. **898**, 336 (1981).
12. T. S. Parker and L. O. Chua Practical, *Numerical Algorithms for Chaotic Systems* (Springer, 1989).
13. Yu. A. Nagovitsyn, Pis'ma Astron. Zh. **33**, 385 (2007) [Astron. Lett. **33**, 340 (2007)].
14. A. G. Ivakhnenko and Yu. P. Yurachkovskii, *Simulation of Complex Systems by Experimental Data* (Radio i svyaz', Moscow, 1987) [in Russian].
15. Yu. A. Nagovitsyn, Pis'ma Astron. Zh. **31**, 622 (2005) [Astron. Lett. **31**, 557 (2005)].
16. J. C. Ribes and E. Nesme-Ribes, Astron. Astrophys. **276**, 549 (1993).
17. M. M. Katsova, M. A. Livshits, and G. Belvedere, Solar Phys. **216**, 353 (2003).
18. Yu. A. Nagovitsyn, Astrofiz. Byull. **63**, 45 (2008).
19. E. V. Miletskii and V. G. Ivanov, Astron. Zh. **86**, 922 (2009) [Astron. Rep. **53**, 857 (2009)].

Translated by G. Rudnitskii